JGR Solid Earth

RESEARCH ARTICLE
10.1029/2020JB020585

Similarities and Differences in the Rupture Processes of the 1952 and 2003 Tokachi-Oki Earthquakes

Hiroaki Kobayashi[1,2], Kazuki Koketsu[1], Hiroe Miyake[1], and Hiroo Kanamori[3]

[1]Earthquake Research Institute, University of Tokyo, Tokyo, Japan, [2]Now at Kobori Research Complex Inc., Tokyo, Japan, [3]Seismological Laboratory, California Institute of Technology, Pasadena, CA, USA

Key Points:

- Rupture processes of two nearby Tokachi-oki M8-class earthquakes 51 years apart are compared by inversion of seismic and geodetic data
- The two earthquakes have similar large rupture patches at approximately the same locations
- They differ in that one earthquake was preceded by an M_w 6.1 subevent and ruptured another slip patch in an adjacent region

Supporting Information:

- Supporting Information S1

Correspondence to:
H. Kobayashi,
kohiroak@kobori-takken.co.jp

Citation:
Kobayashi, H., Koketsu, K., Miyake, H., & Kanamori, H. (2021). Similarities and differences in the rupture processes of the 1952 and 2003 Tokachi-oki earthquakes. *Journal of Geophysical Research: Solid Earth*, *126*, e2020JB020585. https://doi.org/10.1029/2020JB020585

Received 13 JUL 2020
Accepted 15 DEC 2020

Abstract We investigated the similarities and differences between the rupture processes of the 1952 and 2003 Tokachi-oki earthquakes ($M_w \sim 8$) that occurred 51 years apart in the southernmost region of the Kuril subduction zone. This event pair is rare because seismic waveforms of both events were instrumentally recorded. We performed joint source inversion analyses of both earthquakes to better understand the rupture processes of this earthquake sequence. The dataset for the 1952 earthquake consists of teleseismic and strong motion data which were obtained by digitizing copies of analog seismograms. Two datasets were made for the 2003 earthquake to examine the effect of data limitation and to facilitate a comparison of the inversion results of the two earthquakes. One dataset consists of a large amount of teleseismic, strong motion, and geodetic data. The other dataset is similar to that of the 1952 earthquake. Our results show that the rupture propagation, slip areas, and maximum slip amounts were similar for the 1952 and 2003 earthquakes in the Tokachi-oki region. However, there are two important differences: the 1952 earthquake was initiated by an M_w 6.1 subevent in the Tokachi-oki region, and its rupture extended to the adjacent Akkeshi-oki region. The similarity in the rupture pattern of the M8-class earthquake pair suggests the persistence of asperities on the plate interface, while the differences imply a degree of variability in the initiation and termination of the cascading rupture process.

1. Introduction

Investigating the event-to-event slip behavior of great ($M_w \sim 8$) to megathrust ($M_w \sim 9$) interplate earthquakes in the same region is important to understand the physics of earthquake ruptures. Recent great to megathrust events such as the 2011 M_w 9.1 Tohoku earthquake and the 2014 M_w 8.2 Iquique earthquake were captured by dense and high-quality seismic and geodetic observation networks, and the rupture processes of these earthquakes were extensively investigated using various datasets (e.g., Gusman et al., 2015; Ide et al., 2011; Koper et al., 2011; Schurr et al., 2014; Yokota et al., 2011). However, the intervals of great to megathrust interplate earthquakes are generally several decades to several hundreds of years and instrumental seismic observations started at the end of the 19th century and in the early 20th century. As a result, there are only a few great earthquake pairs that have occurred in the same regions and whose waveforms were recorded by seismographs; consequently, detailed comparative studies of such events have been difficult.

Schwartz (1999) compared the locations of asperities, high stress areas with large co-seismic slip (Lay & Kanamori, 1980), of great earthquakes in four subduction zones and suggested that the rupture patterns of great earthquakes are variable. Nagai et al. (2001) performed source inversions of the 1968 M_w 8.3 Tokachi-oki earthquake and the 1994 M_w 7.7 Sanriku-haruka-oki earthquake. They showed that the 1994 Sanriku-haruka-oki earthquake re-ruptured one of the asperities of the 1968 Tokachi-oki earthquake with a variable slip amount. Park and Mori (2007) investigated five great earthquakes along the New Britain Trench and suggested that the asperities were not persistent in this region. Studies of recent great earthquakes, such as the 2015 M_w 8.3 Illapel earthquake and the 2016 M_w 7.8 Ecuador earthquake, showed a partial re-rupture and a quasi-repeat of past earthquakes (Tilmann et al., 2016; Ye et al., 2016).

In the southernmost part of the Kuril subduction zone including the Tokachi-oki, Akkeshi-oki and Nemuro-oki regions (Figure 1a), the Pacific Plate is subducting beneath the North America or Okhotsk Plate with a convergence rate of approximately 8.5 cm/y (Drewes, 2009). We followed the definition of the three regions given in Satake et al. (2005). Note that the division of the zone given in the Headquarters for

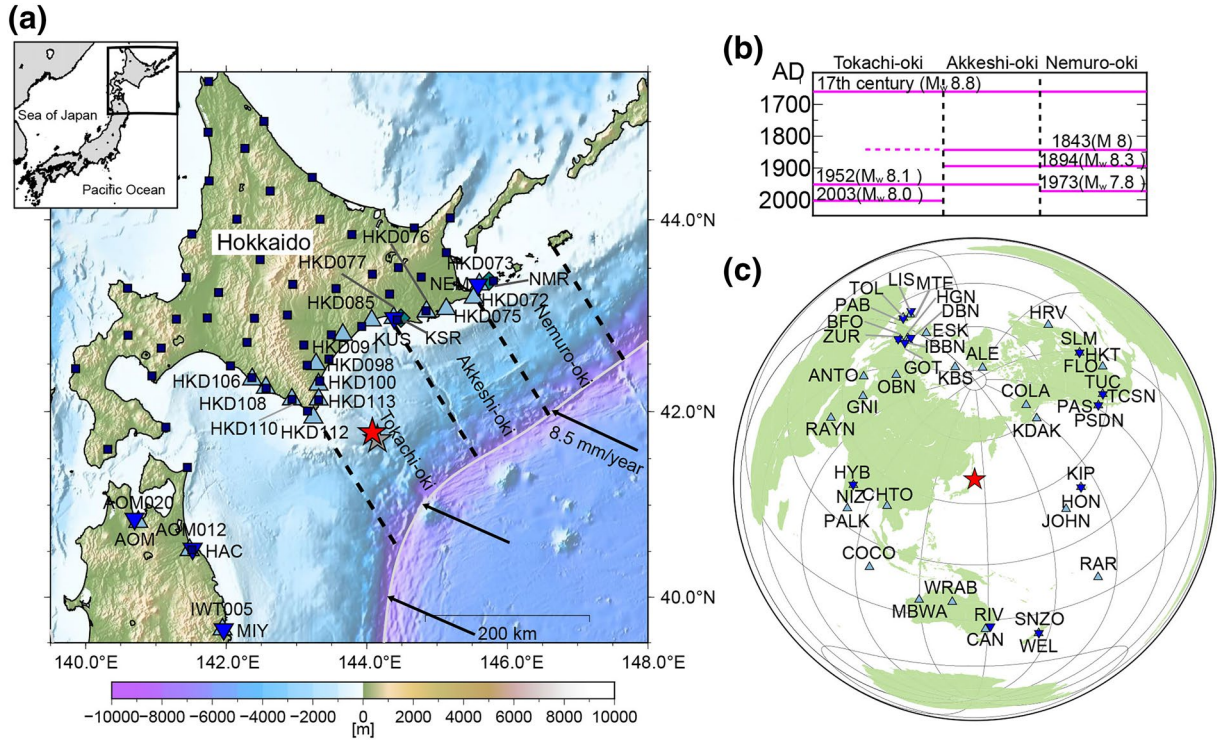

Figure 1. (a) Index map. The black rectangle in the inset represents the map area. The gray and red stars denote the epicenters of the 1952 (41.7057°N, 144.1512°E) and 2003 (41.7785°N, 144.0785°E) Tokachi-oki earthquakes, respectively, as determined by the Japan Meteorological Agency. The blue inverted triangles and sky-blue triangles indicate the strong motion stations in 1952 and 2003, respectively. The blue-green diamonds show the F-net stations. The dark blue squares indicate the Global Navigation Satellite System(GNSS) Earth Observation Network System stations. The black broken lines divide the regions of the southernmost part of the Kuril subduction zone. The gray line shows the trench axis (Iwasaki et al., 2015). The black arrows indicate the motion of the Pacific Plate relative to the North America Plate (Drewes, 2009). The background colors show the topography of the General Bathymetric Chart of the Oceans 2014 (Weatherall et al., 2015). (b) Tsunami source area of the historical earthquakes along the southernmost part of the Kuril subduction zone (Satake, 2017). The seismic moments are from Ioki and Tanioka (2016), Satake et al. (2006), Tanioka et al. (2007), Tanioka, et al. (2004) and Utsu, (1999). (c) Teleseismic station map. The blue inverted triangles and sky-blue triangles indicate the teleseismic stations for the 1952 and 2003 earthquakes, respectively.

Earthquake Research Promotion (2017) is slightly different from that in Satake et al. (2005). In this area, five great earthquakes (Satake, 2017) have occurred in the most recent 200 years (Figure 1b) and another megathrust earthquake occurred in the 17th century (Ioki & Tanioka, 2016; Nanayama et al., 2003; Sawai et al., 2009). In particular, in the Tokachi-oki region, two M8-class earthquakes, the 1952 and 2003 Tokachi-oki earthquakes, occurred in the last 100 years. Therefore, these two M8 event sequences are ideal to investigate the event-to-event slip behavior of great earthquakes.

The 2003 earthquake was recorded by various observation networks and many studies on the source of this earthquake have been conducted using various datasets (Honda et al., 2004; Koketsu et al., 2004; Miura et al., 2004; Miyazaki, Larson, et al., 2004; Romano et al., 2010; Tanioka, Hirata, et al., 2004; Yagi, 2004; Yamanaka & Kikuchi, 2003). All these studies share a common result in that the 2003 earthquake ruptured only the Tokachi-oki region. However, the source studies of the 1952 earthquake indicate some similarities of the 1952 and 2003 ruptures, but also some differences.

Hamada and Suzuki (2004) investigated the aftershocks and seismic intensity distributions of the 1952 Tokachi-oki earthquake, and Nishimura (2006) performed a source inversion using geodetic survey data. These two studies concluded that the 1952 earthquake ruptured only the Tokachi-oki region. Yamanaka and Kikuchi (2003) performed a strong motion inversion of the 1952 earthquake and a teleseismic inversion of the 2003 earthquake. Even though most of the strong motion data for the 1952 earthquake went off scale after the S-wave arrival and the data length was not sufficient, they suggested that the two earthquakes share at least a common rupture area in the Tokachi-oki region. Hartzell and Heaton (1985) estimated the source time functions of various great earthquakes including the 1952 earthquake using teleseismic waveforms

recorded in Pasadena. They found that the moment rate function of the 1952 Tokachi-oki earthquake had two peaks indicating that it was a multiple event. All of the above-mentioned studies on the 1952 earthquake used the seismic and geodetic data and suggest a rupture in the Tokachi-oki region.

Tsunami analyses of the 1952 earthquake have suggested another feature of this event. Tanioka, Nishimura, et al. (2004) compared the observed tsunami runup heights of the 1952 and 2003 earthquakes. They showed that runup heights on the coast of the Tokachi-oki region were similar for the 1952 and 2003 earthquakes but that the runup in the Akkeshi-oki region was larger for the 1952 earthquake than for the 2003 earthquake. Hirata et al. (2003) and Satake et al. (2006) performed source inversions using the tsunami waveforms. Their results indicate that the rupture area of the 1952 earthquake was larger than that of the 2003 earthquake and extended to the Akkeshi-oki region. Hirata et al. (2007) examined the tsunami source area of the 1952 earthquake based on eyewitness testimonies and concluded that the rupture area of the 1952 earthquake reached the Akkeshi-oki region. These tsunami studies suggest that the 1952 earthquake ruptured both the Tokachi-oki and Akkeshi-oki regions.

In this study, we performed source inversions of the 1952 and 2003 Tokachi-oki earthquakes and examined the similarities and differences between the two events. Previous source studies of the 1952 earthquake using the tsunami waveforms did not consider the entire temporal evolution of the rupture process. The temporal and spatial rupture process of the 1952 earthquake has already been studied by Yamanaka and Kikuchi (2003). However, as noted above, the entire rupture process was not analyzed due to the limited data length. Accordingly, we used both teleseismic and strong motion data with sufficient lengths. There have been numerous source studies of the 2003 earthquake; however, detailed parameters such as the maximum slip and seismic moment show large variations between these studies. This is likely due in part to the different datasets, model settings and analysis methods. We performed source inversions of the 1952 and 2003 earthquakes using the same methods and fault models. Because the amount of data is limited for the 1952 earthquake, we made two datasets for the 2003 earthquake, one of which had nearly the same amount of data as the 1952 dataset to maintain the same resolution between the historical 1952 and recent 2003 earthquakes.

2. Data and Method

The distributions of the observation stations are shown in Figures 1a and 1c. For the waveform data of the 1952 earthquake, copies of analog seismograms were collected from the United States Geological Survey, the Japan Agency for Marine-Earth Science and Technology, and the Japan Meteorological Agency (JMA). Moreover, we used the Headquarters for Earthquake Research Promotion data retrieval system of the JMA analog seismograms (http://www.susu.adep.or.jp/#eng; Furumura et al., 2020) and the records printed in Journal of Metrological Agency (1957). These records were manually digitized to obtain the data. We corrected for the arc effect using the method of Kikuchi et al. (1999) when necessary. Parameters of the historical seismographs used in this study are shown in Tables S1 and S2. For the 2003 earthquake, the strong motion data were obtained from K-NET operated by the National Research Institute for Earth Science and Disaster Resilience (2019a). The teleseismic data were obtained from the Incorporated Research Institutions for Seismology Data Management Center (IRIS-DMC). We used coseismic displacement data from the Global Navigation Satellite System (GNSS) Earth Observation Network System stations estimated by Larson and Miyazaki (2008).

Information concerning the time of day is needed to perform source inversions using strong motion data. However, it is often difficult to obtain such information in the case of old seismograms. To address this problem, we picked P-wave arrival times while comparing seismograms of high-gain and low-gain (strong motion) seismographs and assumed that the picked arrival times corresponded to the arrivals reported by the Central Meteorological Observatory (1953). Such comparisons were necessary because the *P*-wave arrival times were often unclear on the low-gain seismograms. We used the origin times determined by JMA: 4 March, 1952 01:22:43.58 for the 1952 earthquake and 25 September, 2003 19:50:07.42 for the 2003 earthquake. The reference time of the teleseismic data in the inversion analysis was the P-wave arrival time. We picked these arrivals for both earthquakes. Even though some waveforms have unclear initial arrivals, we determined the arrival times of these waveforms while considering theoretical arrival times and waveforms

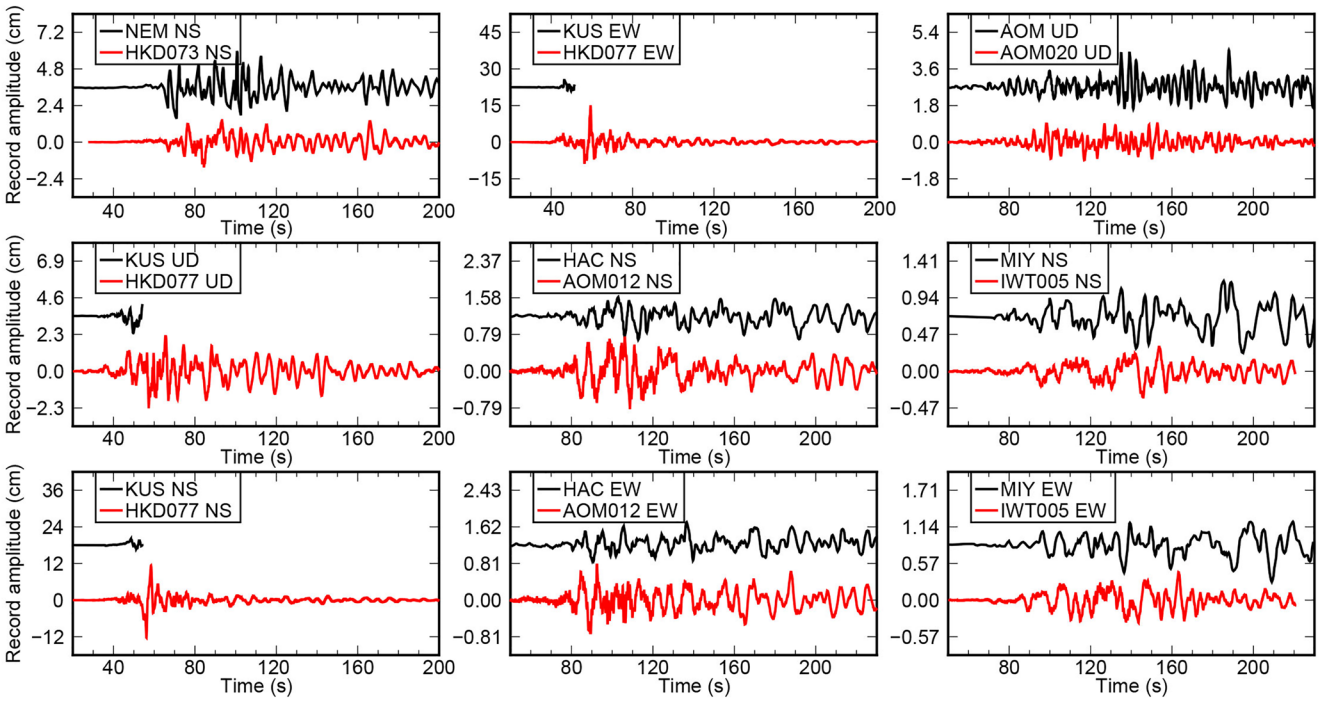

Figure 2. Comparisons of the strong motion waveforms. The black and red lines show the displacement waveforms of the 1952 and 2003 earthquakes, respectively. For each waveform pair, the 2003 waveform is corrected to simulate the 1952 instrument response. The station names and components are shown in each legend. The horizontal axes indicate the time measured from the origin time +7.5 s for the 1952 waveforms and from the origin time for the 2003 waveforms.

with clear initial arrivals. We also used the phase arrival signature written by the operators on those days and the reported arrival times if these were available.

Figures 2–4 show comparisons of the waveforms of the two earthquakes recorded at stations whose locations were close to each other (Figures 1a and 1c). Because the waveforms of the two earthquakes were recorded by different seismographs, we convolved the instrument responses of the old seismographs with the 2003 displacement waveforms for the comparison. In these figures, the reference times (i.e., the origin time or P-wave arrival time) for the 1952 waveforms were shifted left by 7.5 s compared to that of the 2003 waveforms because of the small initial phase, which can be seen only for the 1952 earthquake (Figure 4). As shown in Figures 2 and 3, the waveforms of the two earthquakes have comparable amplitudes, indicating that these two earthquakes had similar magnitudes. However, on some 1952 teleseismic waveforms such as the three components of station DBN and the up-down components of station FLO, there is a large phase near $T = 80$ s (Figure 3) that is not seen in the 2003 waveforms; this second phase is unclear on the strong motion waveforms. Note that we compared the high-gain seismograms and used the waveforms of the F-net (NIED, 2019b) stations (Figure 1a) for the 2003 earthquake (stations KSR and NMR) in Figure 4a because the K-NET record is a trigger-type record and the data length prior to the P-wave arrival is insufficient.

To perform source inversion analyses, we made one dataset (the 1952-S dataset) for the 1952 earthquake and two datasets (the 2003-L and 2003-S datasets) for the 2003 earthquake. The 1952-S dataset consists of the teleseismic P-wave waveforms of 22 components at 12 stations and the strong motion waveforms of nine components at five stations. The 2003-L dataset consists of teleseismic, strong motion, and geodetic data and includes a large amount of data. The 2003-S dataset consists of teleseismic and strong motion data and has nearly the same amount of data and nearly the same station distribution as the 1952-S dataset. The contents of each dataset are summarized in Table 1. Information concerning the teleseismic and strong motion station pairs for the 2003-S and 1952-S datasets is shown in Tables 2 and S3, respectively. In the inversion analyses, all the waveforms were integrated to the displacement, band-pass filtered (non-casual Butterworth) at 0.02–0.2 Hz for the teleseismic waveforms and at 0.05–0.2 Hz for the strong motion

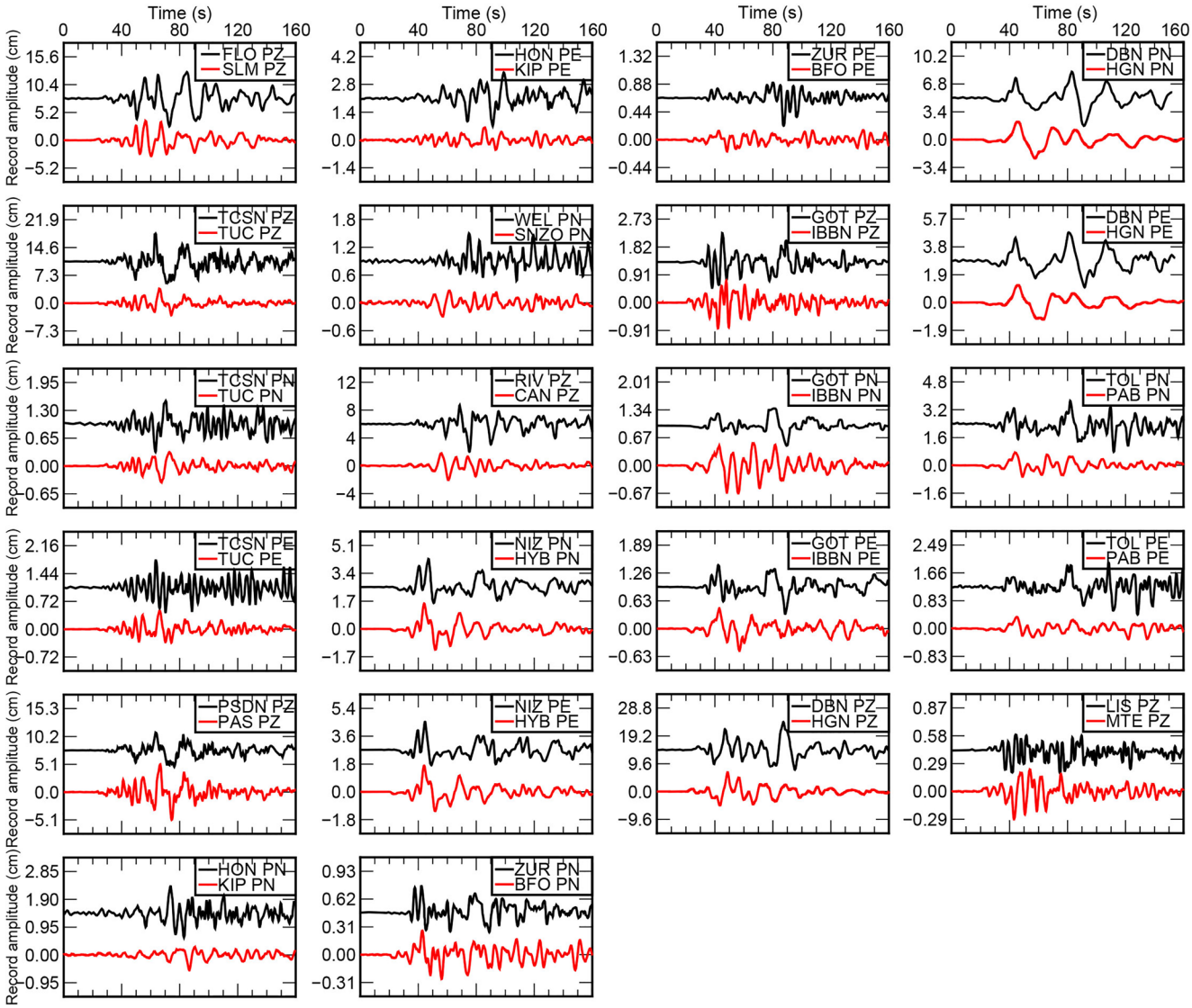

Figure 3. Comparisons of the teleseismic waveforms. The black and red lines show the displacement waveforms of the 1952 and 2003 earthquakes, respectively. For each waveform pair, the 2003 waveform is corrected to simulate the 1952 instrument response. The station names and components are shown in each legend. The time scale is common to all plots. The horizontal axes indicate the time measured from 12.5 s and 20 s prior to the picked P-wave arrival times for the 1952 and 2003 waveforms, respectively.

waveforms, and resampled at 0.5 s intervals. We removed the instrument responses from the teleseismic waveforms.

We used the source inversion method of Hikima and Koketsu (2005) and Yoshida et al. (1996). This method is based on a multi-time-window formulation and solves the linear problem with spatial and temporal smoothness constraints using non-negative least squares. This method minimizes the objective function defined by the model misfit and smoothness, as described in Text S1. We calculated the teleseismic, strong motion, and geodetic Green's functions using the methods of Kikuchi and Kanamori (1991), Kohketsu (1985), and Zhu and Rivera (2002), respectively. To compute the teleseismic Green's functions, we constructed a one-dimensional velocity structure model for the near-source structure (Table S4) from the Japan Integrated Velocity Structure Model (JIVSM; Koketsu et al., 2012). We used the Jeffreys-Bullen model (Bullen, 1963) for the near-receiver structure (Table S5). One-dimensional velocity structure models were extracted from the JIVSM model underneath each station and were used to calculate the strong motion Green's functions.

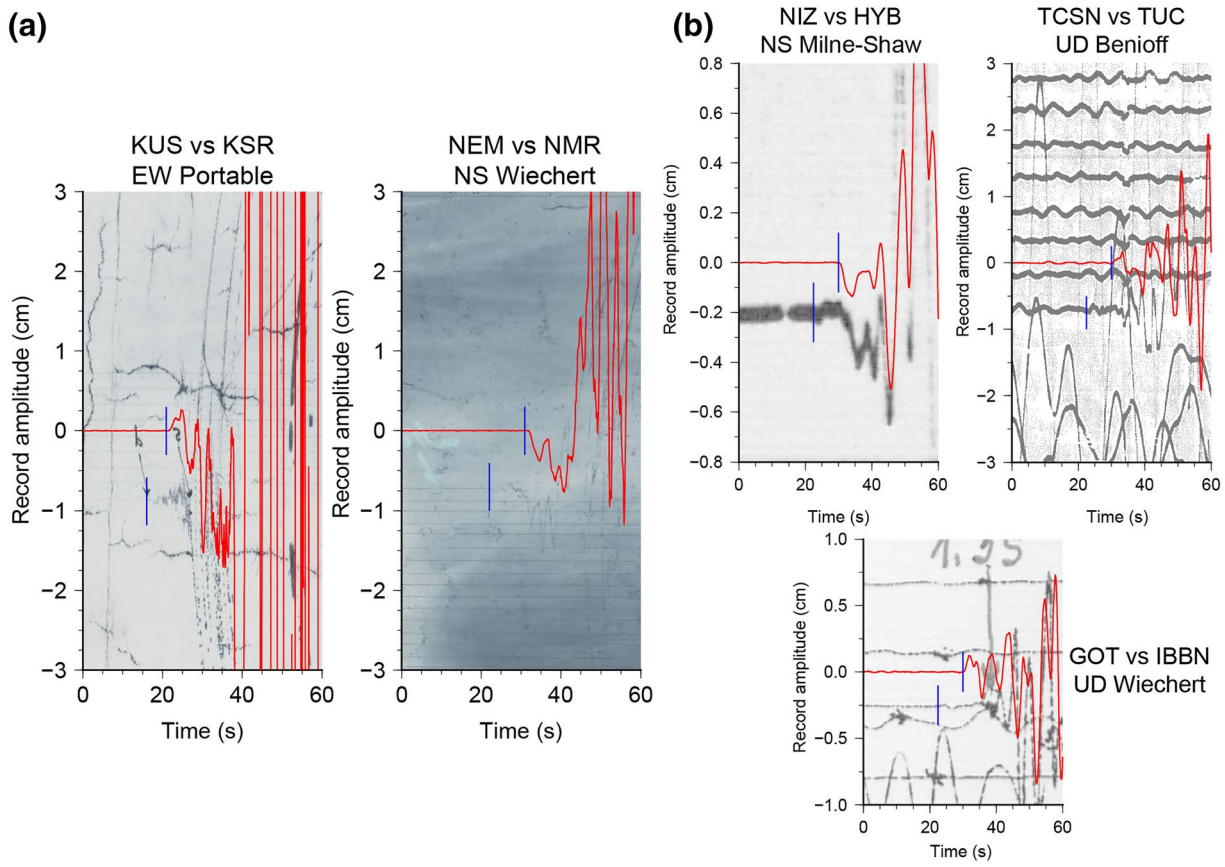

Figure 4. Comparisons of the initial parts of (a) high-gain seismograms at strong motion stations and (b) waveforms at teleseismic stations. The red lines show the waveforms of the 2003 earthquake. The background images show the original waveforms of the 1952 earthquake. The blue lines indicate the first motion arrival times for each event. For each waveform pair, the 2003 waveform is corrected to simulate the 1952 instrument response. The station names, components, and instrument names are shown near each waveform pair. The horizontal axis in panel (a) is the same as that in Figure 2. The horizontal axis in panel (b) indicates the time measured from 22.5 s and 30 s prior to the picked P-wave arrival times for the 1952 and 2003 waveforms, respectively.

The instrumental responses were convolved with the strong motion Green's functions in the inversion analyses using the 1952-S and 2003-S datasets. Because geodetic Green's functions are less sensitive to the velocity structure model than waveform Green's functions, we used the same one-dimensional velocity structure model constructed from JIVSM for all of the geodetic stations (Table S6). We assumed that the basis source time function for each time window is a boxcar function whose duration was 5 s and that the rake angle is allowed to vary between 110 ± 45°. We used the same data weighing method and spatial and temporal smoothness constraints for the 2003-S and 1952-S datasets (see Text S1 for details).

Considering the 1-week aftershock distributions of the two earthquakes, we constructed the fault model shown in Figure 5. The hypocentral depths of the 1952 and 2003 Tokachi-oki earthquakes determined by JMA were 52 km and 45 km, respectively, and are a few tens of kilometers deeper than the plate-boundary depth in the model of Iwasaki et al. (2015) (Figure 5a). In the JMA catalog, due to the lack of stations above the hypocenters, the offshore earthquakes around the 2003 earthquake tend to be mapped deeper than the depths determined using ocean bottom seismometers (Shinohara et al., 2004; Yamada et al., 2005). Therefore, we assumed that the hypocenters of the two earthquakes were located at the plate boundary and fit the fault model accordingly (Figures 5b and 5c). We divided the fault into 17 × 13 subfaults whose fault sizes are 15 km × 15 km. Because the horizontal distance between the hypocenters of the two earthquakes (~10 km) is close to the subfault size, we used the same fault model for the two earthquakes, that is, the locations of the subfaults where the rupture was initiated are different for the two earthquakes.

Table 1
Number of Stations and Components of the Data Used in the Inversion Analyses

			Geodetic	
Dataset	Teleseismic	Strong motion	Horizontal	Vertical
2003-L	27 stations 27 components	17 stations 51 components	52 stations 52 components (GNSS)	23 stations 23 components (GNSS)
2003-S	12 stations 22 components	5 stations 9 components	Not used	Not used
1952-S	12 stations 22 components	5 stations 9 components	Not used	Not used

3. Results

First, we performed a source inversion using the 2003-L dataset. We set four time windows for each subfault and determined the rupture front velocity, V_r, which controls the start times of the first time windows of each subfault. We estimated V_r to be 3.3 km/s by minimizing the data misfit over a V_r range of 1.5–4.5 km/s. The obtained slip distribution indicates that the maximum slip of 7.5 m was located in the Tokachi-oki region and that the rupture primarily propagated in the down-dip direction from the rupture initiation point (Figures 6a and 6b). At 30–60 s from onset, a rupture propagation in the northeastern direction can be seen in the down-dip region. If we set the main rupture area in the Tokachi-oki region as shown by the light gray rectangle in Figure 6a, the seismic moment in the area is 1.7×10^{21} Nm, which yields an M_w of 8.1.

Next, we performed a source inversion using the 2003-S dataset. We re-determined the rupture front velocity to be 2.8 km/s in the same manner as for the 2003-L model and set the same number of time windows. As shown in Figures 6c and 6d, the maximum slip of 6.9 m was located in the Tokachi-oki region and the rupture primarily propagated in the down dip direction from the rupture initiation point. The seismic moment of the main rupture area in the Tokachi-oki region is 1.7×10^{21} Nm (M_w 8.1).

Finally, we performed a source inversion using the 1952-S dataset. We set four time windows and determined the rupture front velocity to be 2.5 km/s using the same method as for the 2003-L datasets. The obtained slip distribution indicates that there were two large slip peaks of 6.9 m and 6.0 m in the Tokachi-oki and Akkeshi-oki regions, respectively (Figure 6e). The rupture primarily propagated from the rupture initiation point in the down-dip direction and then in the northeastern direction, which, in this case, led to another large slip in the Akkeshi-oki region (Figures 6e and 6f). If we set the main rupture area in the Akkeshi-oki region as shown in the gray rectangle in Figure 6e, the seismic moment for the area is 1.1×10^{21} Nm (M_w 8.0). The seismic moment of the main rupture area in the Tokachi-oki region is 1.6×10^{21} Nm (M_w 8.1). Therefore, the total seismic moment for the two main rupture areas is 2.7×10^{21} Nm (M_w 8.2). In all three inversions, the overall fit of the synthetic to the observed data is satisfactory (Figures 7, 8a, 8b, S2, and S3). The resulting parameters of the three inversions are summarized in Table 3. The moment rate functions, calculated by treating the fault model as a plane (i.e., with the strike and dip angles the same for all the subfaults), are shown in Figure S4.

4. Discussion

Both the 2003-L and 2003-S models show the rupture propagation in the down dip direction. However, the rupture front velocity of the 2003-L model is slightly faster than that of the 2003-S model. This is likely due to the small number of strong motion stations in the 2003-S dataset. Nevertheless, the maximum slip locations of the 2003-L and 2003-S models are nearly the same, indicating that the 2003-S and 1952-S datasets are sufficient to obtain the rough rupture processes. However, a peak slip larger than 4 m was obtained for the 2003-S model near the trench region (Figure 6c). The synthetic waveforms from the near trench slip primarily explain the later phases of the observed waveforms (Figure S5). The tsunami source area estimated from tsunami travel time (Hirata et al., 2004) and the slip distribution estimated from tsunami data (Tanioka, Hirata, et al., 2004) do not support the existence of such a slip near the trench. Recently, Lay and Rhode (2019) and Lay et al. (2019) suggested that teleseismic P_{coda} amplitude relative to P amplitude is useful for evaluating up dip extent of rupture because P_{coda} amplitude is relatively large due to water

Table 2
Information Concerning the Teleseismic Station Pairs

2003						1952					
Station	Lat. (°)	Lon. (°)	Azimuth (°)	Back azimuth (°)	Distance (°)	Station	Lat. (°)	Lon. (°)	Azimuth (°)	Back azimuth (°)	Distance (°)
SLM	38.636	−90.236	39.517	−37.407	85.927	FLO	38.802	−90.370	39.541	−37.580	85.753
TUC	32.310	−110.785	56.226	−47.175	79.182	TCSN	32.247	−110.835	56.333	−47.279	79.188
PAS	34.148	−118.171	58.988	−50.559	73.308	PSDN	34.148	−118.172	59.009	−50.654	73.298
KIP	21.420	−158.012	94.145	−53.031	52.322	HON	21.303	−158.095	94.318	−53.040	52.269
SNZO	−41.309	174.704	157.480	-22.348	87.227	WEL	−41.288	174.767	157.478	-22.369	87.138
CAN	−35.319	148.996	175.887	-3.758	76.857	RIV	−33.829	151.158	174.000	−5.390	75.442
HYB	17.417	78.553	−92.647	51.327	60.442	NIZ	17.432	78.454	−92.475	51.424	60.558
BFO	48.330	8.330	−27.951	31.718	82.136	ZUR	47.369	8.580	−28.559	31.802	82.954
IBBN	52.306	7.759	−25.516	31.693	78.943	GOT	51.550	9.967	−27.057	33.101	78.938
HGN	50.764	5.932	−25.333	30.295	80.855	DBN	52.102	5.177	−24.193	29.874	80.023
PAB	39.545	−4.350	−23.867	23.034	94.119	TOL	39.881	−4.049	−23.898	23.212	93.806
MTE	40.400	−7.544	−21.271	20.808	94.246	LIS	38.717	−9.149	−20.640	19.711	96.341

Note. World Geodetic System coordinates are used.

reverberations under deep water when near trench slip exists. They showed that the 2003 earthquake has low P_{coda}/P amplitude, indicating that there is no large near trench slip. Considering the above, this near trench slip is likely an artifact due to inaccurate Green's functions resulting from the use of the one-dimensional velocity structure models and the limited amount of data. Even though a ∼2-m slip zone in the 2003-L model (Figure 6a) and a ∼3-m slip zone in the 1952-S model (Figure 6e) can be seen at the same location, these features may be poorly resolved.

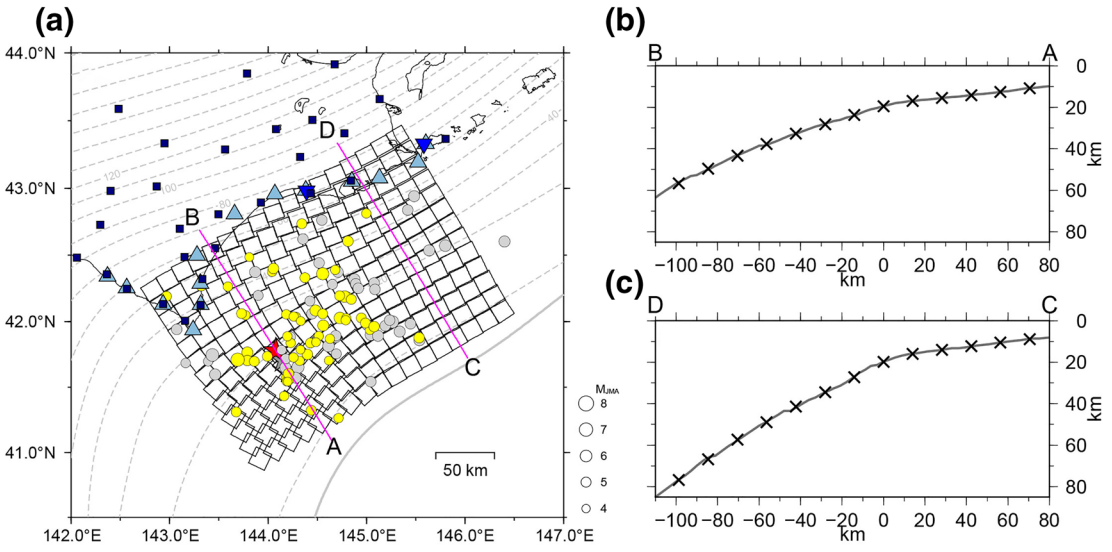

Figure 5. (a) Fault model used in the inversion analyses. The black lines show the fault model. The light gray and yellow circles indicate the one-week aftershocks of the 1952 and 2003 earthquakes ($M_{JMA} > 4.5$), respectively. The plate-boundary depth and the trench axis (Iwasaki et al., 2015) are represented by the light gray broken lines with 10-km contour intervals and the light gray line, respectively. The purple lines show the locations of the cross sections described in panels (b) and (c). Other aspects are the same as in Figure 1a. (b) and (c) Cross sections along the lines AB and CD in panel (a), respectively. The black crosses denote the locations of the point sources (i.e., the centers of each subfault). The gray lines show the plate boundary (Iwasaki et al., 2015).

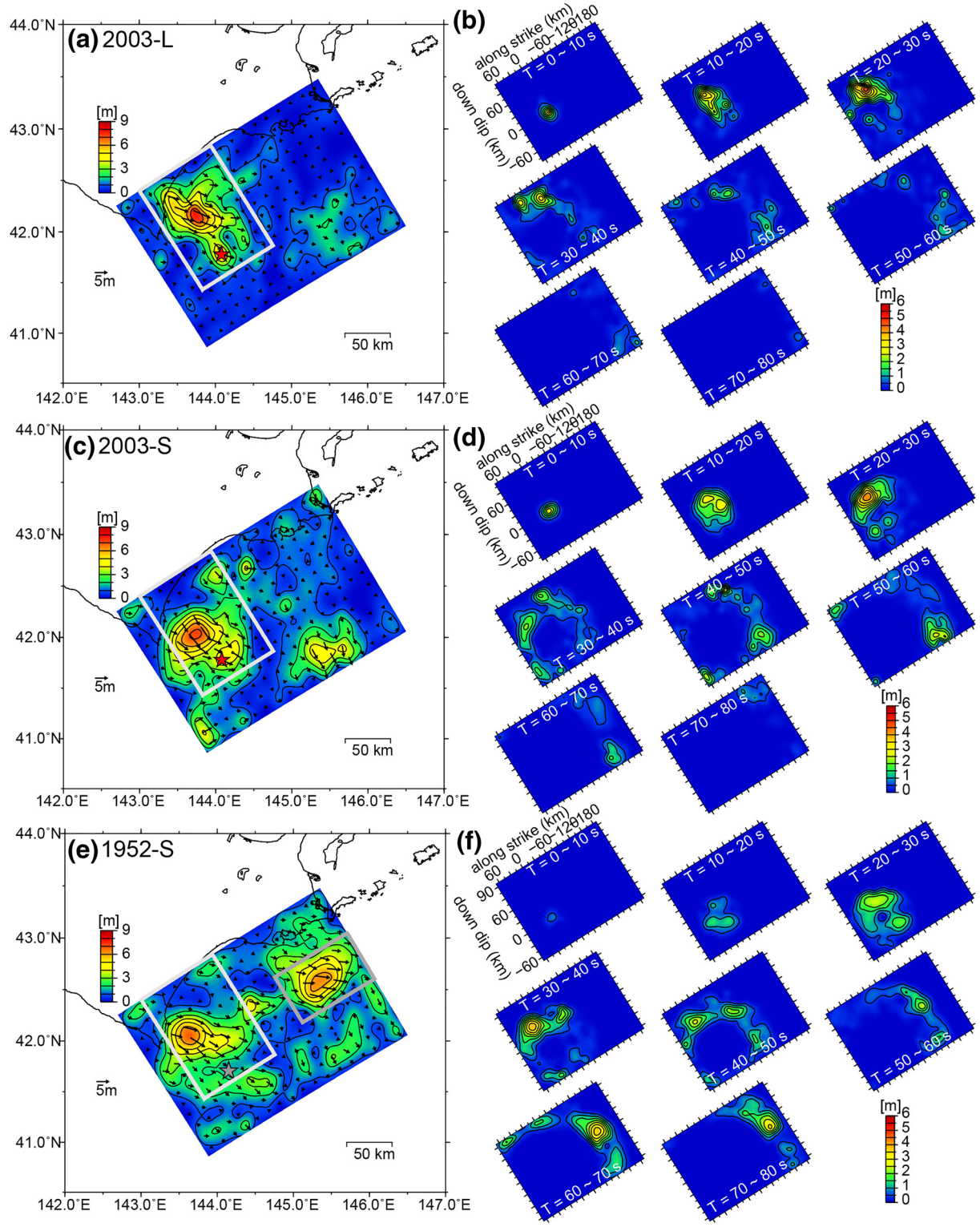

Figure 6. Slip distribution and snapshots of the slip distribution. (a) and (b) The result with the 2003-L dataset. (c) and (d) The result with the 2003-S dataset. (e) and (f) The result with the 1952-S dataset. The contour intervals of the slip distributions and snapshots are 1 m and 0.5 m, respectively. The light gray and gray rectangles represent the main rupture areas in the Tokachi-oki and Akkeshi-oki regions, respectively. The red and gray stars denote the epicenters of the 2003 and 1952 Tokachi-oki earthquakes, respectively.

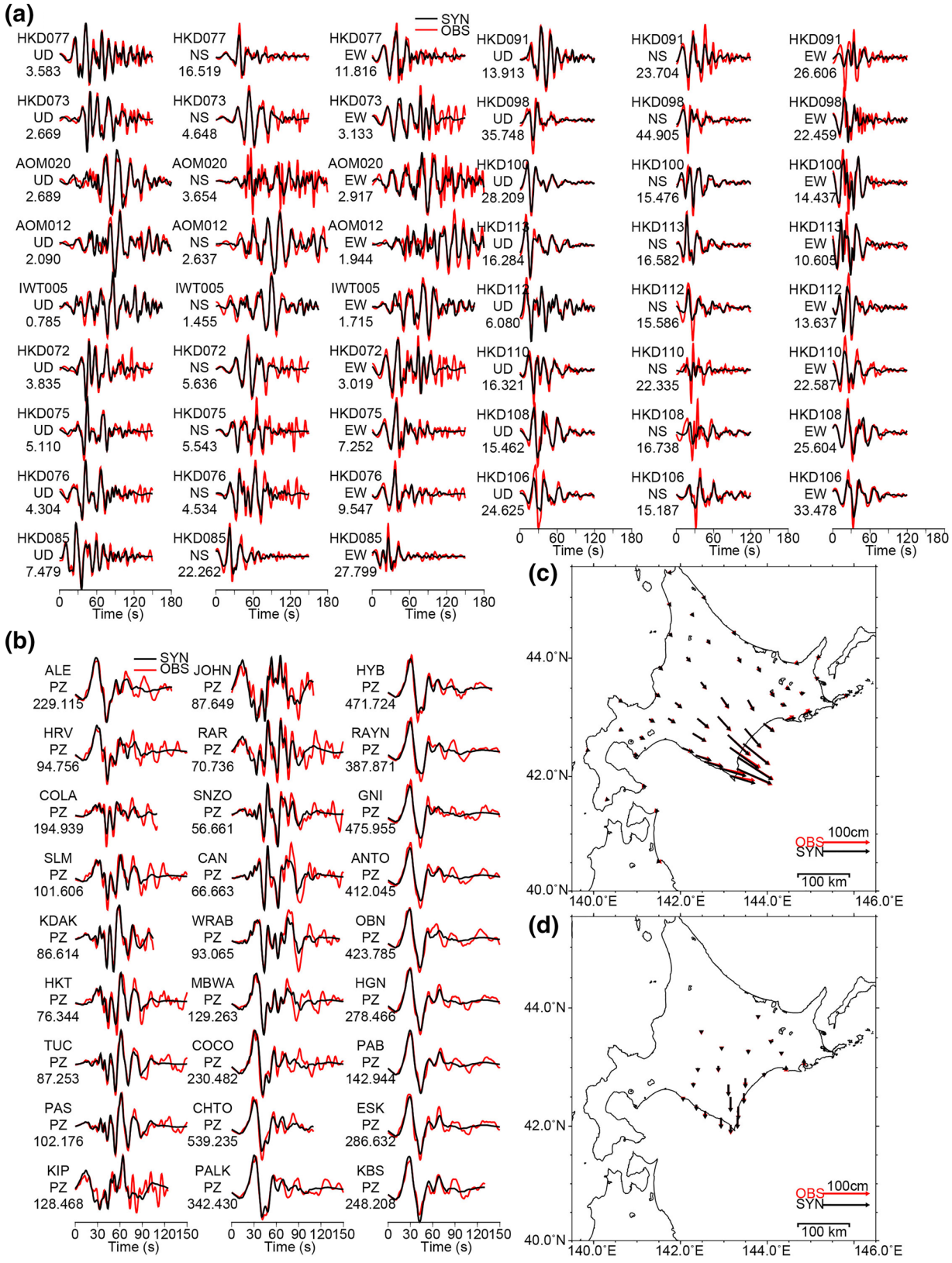

Figure 7. (a) Strong motion, (b) teleseismic, and (c) horizontal and (d) vertical static displacement data fits of the 2003-L dataset. The observed and synthetic data are shown with the red and black lines/arrows, respectively. The station names, components, and maximum amplitude of the observed waveforms (cm for strong motion and μm for teleseismic) are shown to the left of each waveform.

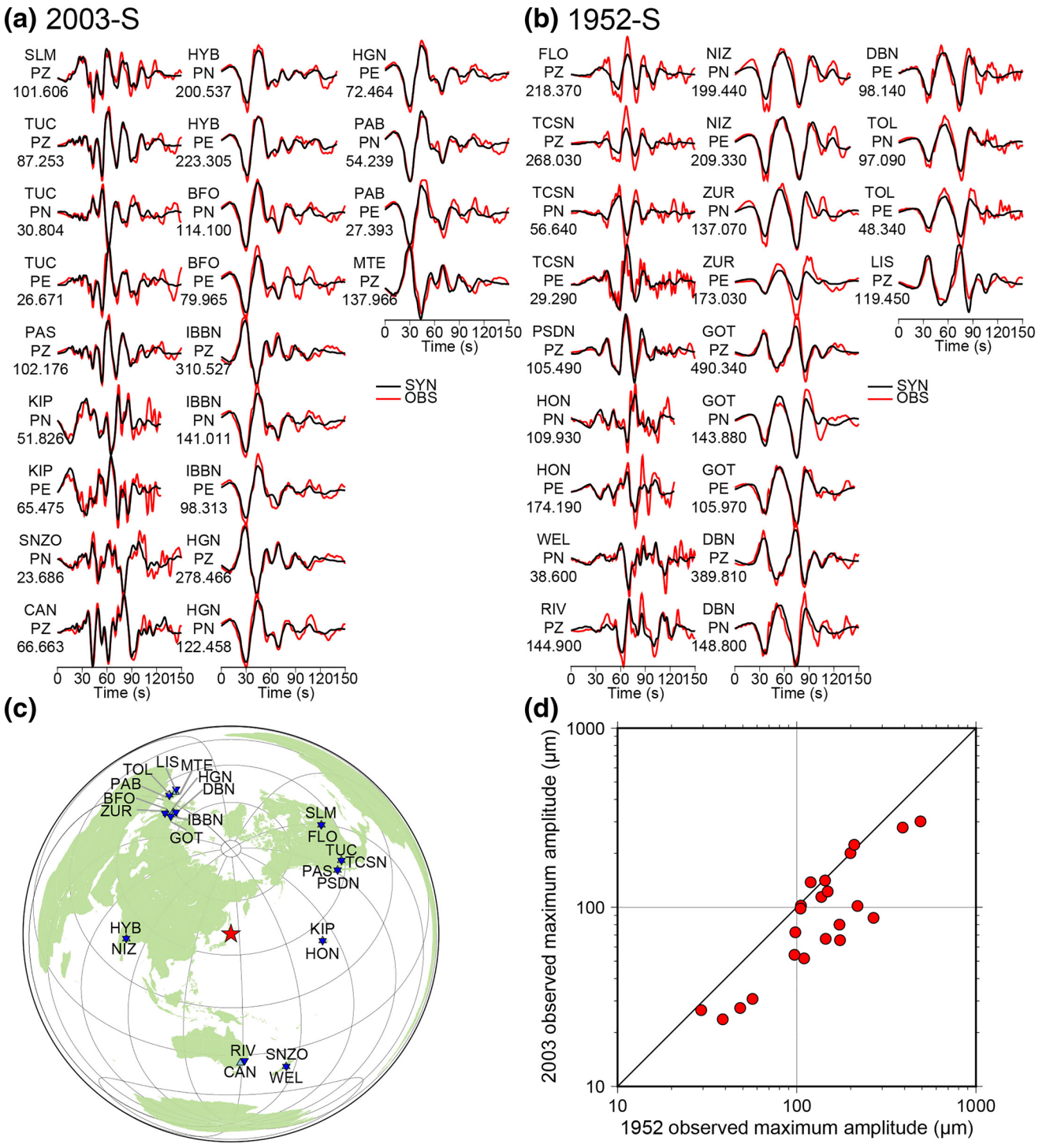

Figure 8. Teleseismic waveform fit of the inversions of the (a) 2003-S and (b) 1952-S datasets. The observed and synthetic displacement waveforms (0.02–0.2 Hz) are shown with the red and black lines, respectively. The station names, components, and maximum amplitudes of the observed waveforms in μm are shown to the left of each waveform. (c) Teleseismic station map simplified from Figure 1c. The red star denotes the epicenter of the 2003 earthquake. The blue inverted triangles and sky-blue triangles indicate the teleseismic stations for the 1952 and 2003 earthquakes, respectively. (d) Comparison of the observed maximum amplitudes of the teleseismic waveform pairs. The red circles indicate the amplitudes of the waveform pairs.

Table 3
Resulting Parameters of the Inversions

		Tokachi-oki		Akkeshi-oki	
Dataset	V_r (km/s)	D_{max} (m)	M_0[a] (Nm)	D_{max} (m)	M_0[a] (Nm)
2003-L	3.3	7.5	1.7×10^{21} (M_w 8.1)	–	–
2003-S	2.8	6.9	1.7×10^{21} (M_w 8.1)	–	–
1952-S	2.5	6.9	1.6×10^{21} (M_w 8.1)	6.0	1.1×10^{21} (M_w 8.0)

V_r: rupture front velocity; and D_{max}: maximum slip amount.
[a]Moment values for the rectangular regions shown in Figure 6.

The source inversion results of the 1952 and 2003 earthquakes using the 1952-S and 2003-S datasets show that both earthquakes had similar rupture propagation, slip areas, and maximum slip amounts in the Tokachi-oki region (Figures 6c–6f). However, the 1952 earthquake also ruptured the Akkeshi-oki region. We believe that the large slip in the Akkeshi-oki region in the 1952-S model is not an artifact because only the teleseismic waveforms of the 1952 earthquake, which were obtained by deconvolution of the instrument response and filtering between 0.02 and 0.2 Hz, have two clear large phases, especially in the waveforms at stations NIZ to LIS (Figure 8), and the moment rate function of the 1952-S model also has two clear peaks (Figure S4), as shown in Hartzell and Heaton (1985). The observed maximum amplitudes of the 1952 teleseismic waveforms are generally larger than those of the 2003 teleseismic waveforms (Figure 8d). This is consistent with the slightly larger total seismic moment of the 1952 earthquake. Comparisons of m_B, the body wave magnitude, and M_S, the surface wave magnitude, for the 1952 and 2003 earthquakes are also consistent with the amplitude differences and the moment rate functions (see Text S2 for details).

The overlapping large slip areas between the 1952 and 2003 earthquakes in the Tokachi-oki region (Figure 9a) suggest the persistence of asperities along this segment of the subduction zone. Park and Mori (2007) suggested non-persistence of asperities along the New Britain Trench because the asperities of the five great earthquakes they analyzed did not overlap. However, the five earthquakes occurred within a much shorter period of time (~30 years) than the expected recurrence period of M8-class earthquakes in the region (~100 years), and their result can be interpreted as ruptures of different asperities for each event.

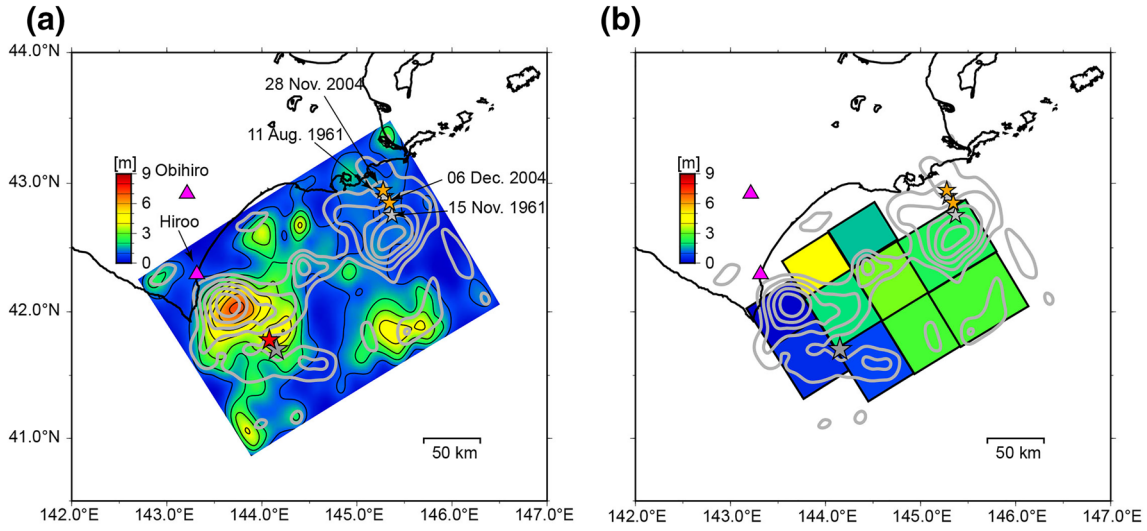

Figure 9. Comparisons between the slip distributions of (a) the 2003-S (background colors) and 1952-S (gray contours) models and (b) the 1952-S model (gray contours, the contours of ≥2 m are plotted) and the tsunami-based model of Satake et al. (2006) (background colors). The contour intervals are 1 m. The large gray and red stars denote the epicenters of the 1952 and 2003 Tokachi-oki earthquakes, respectively. The small gray and orange stars indicate the epicenters of the M7 earthquakes prior to and after the 2003 earthquake, respectively. The epicenter locations are from the Japan Meteorological Agency catalog. The purple triangles indicate the seismic stations for which the observed waveforms of the 1961 and 2004 earthquakes are shown in Figure S7.

The last event that ruptured the Tokachi-oki region prior to 1952 may have been the great earthquake in 1843 (Figure 1b); if this is the case, the two most recent event intervals are 109 and 51 years. If the slip deficit rate is equal to the plate convergence rate (8.5 cm/y) and is constant during the event intervals, the accumulated slip deficits between the two intervals are 9.3 m and 4.3 m, respectively. Even though the maximum slip amount varies greatly in previous studies of the 2003 earthquake, it is between 5 m and 9 m in most of these studies including this study, and the maximum slip of the 1952 earthquake in the Tokachi-oki region is comparable to that of the 2003 earthquake. This suggests that the maximum slip of the 1952 earthquake was less than the accumulated slip deficit since the 1843 event and that the maximum slip of the 2003 earthquake was larger than the accumulated slip deficit since the 1952 earthquake. However, note that, in this calculation, we do not consider the possibility of a temporal change in the slip deficit rate (Loveless & Meade, 2016; Mavrommatis et al., 2014; Yokota & Koketsu, 2015) or stress transfers from surrounding great earthquakes.

Previous source studies of the 1952 earthquake using tsunami data (Hirata et al., 2003; Satake et al., 2006) suggest that the rupture area of the 1952 earthquake extended to the Akkeshi-oki region. Our result is consistent with their results on that point. However, the slip distribution of the tsunami analysis had a slip near the trench (Figure 9b). Azuma et al. (2012) conducted a seismic survey at the near trench region where Satake et al. (2006) suggested ~3-m slip (Figure 9b). Azuma et al. (2012) obtained strong reflectivity on the plate interface in the region indicating a weak interplate coupling and quasi-stable slip conditions. However, because the slip distribution obtained by Hirata et al. (2003) has a large slip of 7 m at the near trench region, Azuma et al. (2012) suggested that the 1952 earthquake had characteristics of a tsunami earthquake. The slip distribution of Satake et al. (2006) which was obtained by using finer grid system than that of Hirata et al. (2003) and correcting the clock errors of the tide gauge stations also shows ~3-m slip in the near trench region (Figure 9b). Because the old seismograms used for the analyses of the 1952 earthquake were good only up to a period of 50 s (0.02 Hz), even if there were slow slips at the near trench region, we cannot measure such slips. However, even though the possibility remains that the 1952 earthquake had some slips at the near trench region, it cannot be a typical tsunami earthquake like the 1946 Unimak Islands (in the Aleutians) earthquake or the 1896 Sanriku, Japan, earthquake. Because the $M_w = 8.2$ for the 1952 earthquake determined from the seismic frequency band is already very large, if it was a typical tsunami earthquake, the tsunamis should have been far more widespread than reported for this event.

No large slip has occurred in the Akkeshi-oki region since the 1952 earthquake because the 2003 earthquake did not rupture the Akkeshi-oki region. However, in the Akkeshi-oki region, two smaller earthquakes, M_{JMA} 7.1 and 6.9, occurred on 28 November and 6 December 2004, respectively, approximately 1 year after the 2003 earthquake (Figure 9). The epicenters of these earthquakes were located near the area where a large slip occurred during the 1952 earthquake. According to the Global Centroid-Moment-Tensor Project (Ekström et al., 2012), the M_w values of these earthquakes are 7.0 and 6.7; therefore, the sum of their seismic moments is far less than the seismic moment of the 1952 earthquake in the Akkeshi-oki region. Moreover, no afterslip occurred after the 2003 earthquake in the Akkeshi-oki region (Baba et al., 2006; Miyazaki, Segall, et al., 2004), indicating that there was no significant strain release in the Akkeshi-oki region after the 2003 earthquake. Between the 1952 and 2003 earthquakes, two earthquakes with M_{JMA} 7.2 and 6.9 occurred on 11 August and 15 November 1961, respectively, ~9 years after the 1952 earthquake (Figure 9). We did not investigate the details of these earthquakes in this paper; however, the similarity of the waveforms recorded at the JMA stations Hiroo and Obihiro (Figure S7) suggests that these two M7 earthquake pairs ruptured nearly the same location and have nearly the same M_w values (the JMA stations Hiroo and Obihiro were at the same locations during time period between 1961 and 2004). No other earthquakes with magnitudes larger than M_{JMA} 7.0 occurred between the 1952 and 2003 earthquakes. Even though the slip deficit rate in the Akkeshi-oki region between the 1952 and 2003 earthquakes is unknown, it is highly likely that strain has accumulated in the Akkeshi-oki region since the 1952 earthquake. The Akkeshi-oki region has been ruptured with the Tokachi-oki and Nemuro-oki regions (Figure 1b). Our result indicates that an earthquake of at least M_w 8 could occur independently in the Akkeshi-oki region.

The source inversions cannot satisfactorily resolve the small initial rupture of the 1952 earthquake due to the small amplitude and short duration of this small initial phase (Figures 4, 6e, and 6f). Therefore, we examined this small initial rupture in detail separately. We estimated the first motion solution of the 1952

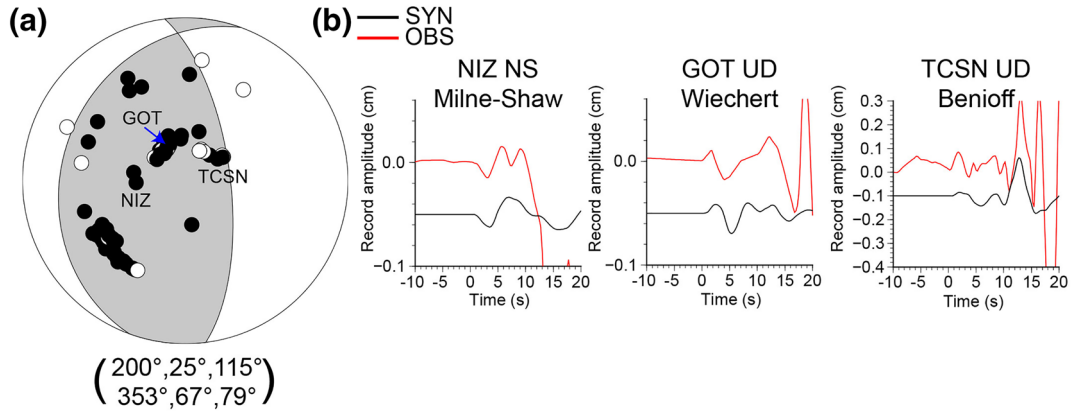

Figure 10. (a) Estimated P-wave first motion solution for the 1952 earthquake. The black and white circles indicate the reported compressional and dilatational first motions, respectively. The fault plane solutions (strike, dip, and rake) are shown below the focal mechanism. (b) The observed and synthetic waveforms (0.25-s sampled and band-passed between 0.001 Hz and 1.0 Hz). The instrument responses were convolved to the synthetic waveforms. The waveforms are plotted for an initial arrival of $T = 0$ s. The station names and components are given above each plot.

earthquake using polarity data that were determined in this study as well as reported to the International Seismological Centre and JMA. To plot the polarity data we calculated the takeoff angles using the 1D JMA2001 velocity structure model (Ueno et al., 2002) for the stations whose epicentral distances were less than 2,000 km and the Preliminary Reference Earth Model (Dziewonski et al., 1981) for the teleseismic stations whose epicentral distances were between 35° and 95°. Because the polarity data may include errors due to various causes such as incorrect assessments by the analyst and noisy seismogram traces, we determined a plausible solution via trial and error (Figure 10). We then used the first motion mechanism to calculate the synthetic waveforms using the same method as that used in the inversion analysis and convolved this with the instrumental response. We found that the initial phase of the waveforms can be reproduced well by assuming an isosceles triangle source time function with a width of 5.5 s and a seismic moment of 1.8×10^{18} Nm (M_w 6.1). This duration was calculated using Equation 1 in Ekström et al. (2012). The rupture area of the M_w 6.1 earthquake was approximately 200 km^2 according to the scaling relationship for interplate earthquakes (Murotani et al., 2008; 2013). Therefore, the fault width of the M_w 6.1 earthquake was 14 km if the fault width was equal to the fault length, or 10 km if the width was half the length. These values are close to the horizontal distance between the hypocenters of the 1952 and 2003 earthquakes.

The 1952 earthquake was initiated by a M_w 6.1 subevent, ruptured the Tokachi-oki region, and cascaded into the adjacent Akkeshi-oki region. Large afterslip occurred in the boundary region between the Tokachi-oki and Akkeshi-oki regions after the 2003 earthquake. Miyazaki, Segall, et al. (2004) suggested different frictional properties between the co-seismic slip and afterslip areas. The different rupture patterns of the 1952 and 2003 earthquakes suggest that the boundary region with velocity strengthening frictional property sometimes prohibits rupture growth into an adjacent region. Accumulated strain level in the adjacent region should also be an important factor for rupture growth. One possible explanation for the difference in the rupture initiations of the 1952 and 2003 earthquakes is a complex rough structure on the fault plane. The existence of hierarchical structures which consist of circular patches with various diameters proportional to the fracture energy (e.g., Ide & Aochi, 2005) could be another possible explanation. Noda et al. (2013) performed numerical simulations assuming a simple hierarchical structure consisting of large and small patches. They showed that a rupture of the large patch could be initiated by either a large nucleation zone in the large patch or a cascading rupture of the small patches.

Ioki and Tanioka (2016) estimated the seismic moment of the megathrust earthquake in the 17th century to be 1.7×10^{22} Nm (M_w 8.8). They estimated a fault model with 10-m slip in the Tokachi-oki region, 5-m slip in the Akkeshi-oki and Nemuro-oki regions, and 25-m slip extending over the three very-near-trench regions to explain the tsunami deposits. The 10-m slip in the Tokachi-oki region may be larger than the average slip of the M8 earthquakes in this region because their model assumes uniform slip over the entire Tokachi-oki

region. Our source inversion results show that the 1952 earthquake ruptured both the Tokachi-oki and Akkeshi-oki regions but that the slip amount in the Tokachi-oki region was similar to that of the 2003 earthquake, which only ruptured the Tokachi-oki region. This suggests that the slip in the Tokachi-oki region does not necessarily increase when the rupture cascades into an adjacent region, but might increase when the near-trench region simultaneously ruptures.

5. Conclusions

We performed joint source inversions of the 1952 and 2003 Tokachi-oki earthquakes ($M_w \sim 8$) to investigate the similarities and differences in the rupture processes between these earthquakes. We performed two inversions for the 2003 earthquake using two datasets to examine the effect of data limitation on the 1952 earthquake and to facilitate a comparison between the two earthquakes. The first is a large dataset consisting of tele-seismic, strong motion, and geodetic data, while second is a smaller dataset consisting of teleseismic and strong motion data. The amount of data in the smaller dataset is nearly the same as that available for the 1952 earthquake. The results of the two inversions of the 2003 earthquake demonstrated that the limited dataset is sufficient to investigate the overall rupture process. The inversion results of the 2003 and 1952 earthquakes revealed similar rupture propagation, slip areas, and maximum slip amounts in the Tokachi-oki region for both earthquakes. However, the 1952 earthquake differed from the 2003 earthquake in that the former also ruptured the Akkeshi-oki region. Comparisons of the teleseismic waveforms for the 2003 and 1952 earthquakes clearly show that the 1952 earthquake was a multiple event. An examination of the initial part of the teleseismic waveforms revealed that the 1952 earthquake was initiated by an M_w 6.1 subevent in the Tokachi-oki region. The similarities between the two earthquakes indicate spatial persistence of asperities on the plate interface, while the differences seen in the rupture initiation and termination imply variability in the cascading rupture behavior.

Data Availability Statement

Some station bulletins were obtained from the SISMOS project (http://storing.ingv.it/bulletins/ISC-GEM/). The waveforms of the JMA stations are provided by the Japan Meteorological Business Support Center (http://www.jmbsc.or.jp/en/index-e.html). The teleseismic data were provided by the Wilber three system of IRIS-DMC (http://ds.iris.edu/wilber3/find_event). The plate models by Iwasaki et al. (2015) were constructed from topography and bathymetry data by GSI (250-m digital map), Japan Oceanographic Data Center (500 m mesh bathymetry data, J-EGG500, http://www.jodc.go.jp/jodcweb/JDOSS/infoJEGG_j.html) and Geographic Information Network of Alaska, University of Alaska (Lindquist et al., 2004). The copies of the Gutenberg notepad used in this study are provided by the Archives of the California Institute of Technology. The digitized data used in this paper can be downloaded from the Zenodo data repository (http://doi.org/10.5281/zenodo.3941018). Figures were drawn using the General Mapping Tools (Wessel & Smith, 1998).

Acknowledgments
The authors would like to thank Toshitaka Baba, Phil Cummins, Shuichiro Fukumitsu, Willie Lee, Satoko Murotani, Kazuko Noguchi, Toshihiro Shimoyama, Steve Walter, and Yoshiko Yamanaka for their help in collecting and processing the copies of analog seismograms. The authors thank Thorne Lay for reading our manuscript and providing helpful comments and Luis Rivera for helping us identify some of the old observatories listed in the Gutenberg Notepad. The authors also thank two anonymous reviewers for their helpful reviews.

References

Azuma, R., Murai, Y., Katsumata, K., Nishimura, Y., Yamada, T., Mochizuki, K., & Shinohara, M. (2012). Was the 1952 Tokachi-oki earthquake ($Mw = 8.1$) a typical underthrust earthquake?: Plate interface reflectivity measurement by an air gun – Ocean bottom seismometer experiment in the Kuril Trench. *Geochemistry, Geophysics, Geosystems*, *13*, Q08015. https://doi.org/10.1029/2012GC004135

Baba, T., Hirata, K., Hori, T., & Sakaguchi, H. (2006). Offshore geodetic data conducive to the estimation of the afterslip distribution following the 2003 Tokachi-oki earthquake. *Earth and Planetary Science Letters*, *241*, 281–292. https://doi.org/10.1016/j.epsl.2005.10.019

Bullen, K. E. (1963). *An introduction to the theory of seismology*. New York, NY: Cambridge University Press.

Central Meteorological Observatory. (1953). A report of the Tokachi earthquake of March 4, 1952. *Quarterly Journal of Seismology*, *17*, 1–130.

Drewes, H. (2009). The actual plate kinematic and crustal deformation model APKIM2005 as basis for non-rotating ITRF. In H. Drewes (Ed.), Geodetic reference frames (134, pp. 95–99). Berlin: International Association of Geodesy SymposiaSpringer. https://doi.org/10.1007/978-3-642-00860-3_15

Dziewonski, A. M., & Anderson, D. L. (1981). Preliminary reference Earth model. *Physics of the Earth and Planetary Interiors*, *25*, 297–356. https://doi.org/10.1016/0031-9201(81)90046-7

Ekström, G., Nettles, M., & Dziewoński, A. M. (2012). The global CMT project 2004–2010: Centroid-moment tensors for 13,017 earthquakes. *Physics of the Earth and Planetary Interiors*, *200–201*, 1–9. https://doi.org/10.1016/j.pepi.2012.04.002

Furumura, M., Iwasa, K., Suzuki, Y., Demachi, T., Ishibe, T., & Matsu'ura, R. S. (2020). Data retrieval system of JMA analog seismograms in the Headquarters for Earthquake Research Promotion of the Japanese Government. *Seismological Research Letters*, *91*, 1403–1412. https://doi.org/10.1785/0220190303

Gusman, A. R., Murotani, S., Satake, K., Heidarzadeh, M., Gunawan, E., Watada, S., & Schurr, B. (2015). Fault slip distribution of the 2014 Iquique, Chile, earthquake estimated from ocean-wide tsunami waveforms and GPS data. *Geophysical Research Letters*, *42*, 1053–1060. https://doi.org/10.1002/2014GL062604

Hamada, N., & Suzuki, Y. (2004). Re-examination of aftershocks of the 1952 Tokachi-oki earthquake and a comparison with those of the 2003 Tokachi-oki earthquake. *Earth Planets and Space*, *56*, 341–345. https://doi.org/10.1186/BF03353062

Headquarters for Earthquake Research Promotion. (2017). *Long-term evaluation of occurrence potentials of subduction-zone earthquakes along the Kuril trench, the third edition*, Headquarters for Earthquake Research Promotion. Retrieved from https://www.jishin.go.jp/main/chousa/kaikou_pdf/chishima3.pdf

Hertzell, S. H., & Heaton, T. H. (1985). Teleseismic time functions for large, shallow subduction zone earthquakes. *Bulletin of the Seismological Society of America*, *75*, 965–1004.

Hikima, K., & Koketsu, K. (2005). Rupture process of the 2004 Chuetsu (mid-Niigata prefecture) earthquake, Japan: A series of events in a complex fault system. *Geophysical Research Letters*, *32*, L18303. https://doi.org/10.1029/2005GL023588

Hirata, K., Geist, E., Satake, K., Tanioka, Y., & Yamaki, S. (2003). Slip distribution of the 1952 Tokachi-Oki earthquake (*M* 8.1) along the Kuril Trench deduced from tsunami waveform inversion. *Journal of Geophysical Research*, *108*, 2196. http://doi.org/10.1029/2002JB001976

Hirata, K., Satake, K., Yamaki, S., Tanioka, Y., Yamanaka, Y., & Nishimura, T. (2007). Examination of the northeast edge of the 1952 Tokachi-oki earthquake tsunami Source based on eyewitness accounts stated in previously published reports. *Zisin*, *60*, 21–41. https://doi.org/10.4294/zisin.60.21

Hirata, K., Tanioka, Y., Satake, K., Yamaki, S., & Geist, E. L. (2004). The tsunami source area of the 2003 Tokachi-oki earthquake estimated from tsunami travel times and its relationship to the 1952 Tokachi-oki earthquake. *Earth Planets and Space*, *56*, 367–372. https://doi.org/10.1186/BF03353066

Honda, R., Aoi, S., Morikawa, N., Sekiguchi, H., Kunugi, T., & Fujiwara, H. (2004). Ground motion and rupture process of the 2003 Tokachi-oki earthquake obtained from strong motion data of K-NET and KiK-net. *Earth Planets and Space*, *56*, 317–322. https://doi.org/10.1186/BF03353058

Ide, S., & Aochi, H. (2005). Earthquake as multiscale dynamic ruptures with heterogeneous fracture surface energy. *Journal of Geophysical Research*, *110*, B11303. https://doi.org/10.1029/2004JB003591

Ide, S., Baltay, A., & Beroza, G. C. (2011). Shallow dynamic overshoot and energetic deep rupture in the 2011 Mw 9.0 Tohoku-Oki earthquake. *Science*, *332*, 1426–1429. https://doi.org/10.1126/science.1207020

Ioki, K., & Tanioka, Y. (2016). Re-estimated fault model of the 17th century great earthquake off Hokkaido using tsunami deposit data. *Earth and Planetary Science Letters*, *433*, 133–138. https://doi.org/10.1016/j.epsl.2015.10.009

Iwasaki, T., Sato, H., Shinohara, M., Ishiyama, T., & Hashima, A. (2015). *Fundamental structure model of island arcs and subducted plates in and around Japan*. San Francisco, CA: American Geophysical Union Fall Meeting.

Japan Meteorological Agency (1957). Seismograms of strong earthquakes in Japan, 1923-1956. *Quarterly Journal of Seismology Supplementary*, *22*, 1–136.

Kikuchi, M., & Kanamori, H. (1991). Inversion of complex body waves—III. *Bulletin of the Seismological Society of America*, *81*, 2335–2350.

Kikuchi, M., Nakamura, M., Yamada, M., & Yoshikawa, K. (1999). Source parameters of the 1948 Fukui earthquake inferred from low-gain strong-motion records. *Zisin*, *52*, 121–128. https://doi.org/10.4294/zisin1948.52.1_121

Kohketsu, K. (1985). The extended reflectivity method for synthetic near-field seismograms. *Journal of Physics of the Earth*, *33*, 121–131. https://doi.org/10.4294/jpe1952.33.121

Koketsu, K., Hikima, K., Miyazaki, S., & Ide, S. (2004). Joint inversion of strong motion and geodetic data for the source process of the 2003 Tokachi-oki, Hokkaido, earthquake. *Earth Planets and Space*, *56*, 329–334. https://doi.org/10.1186/BF03353060

Koketsu, K., Miyake, H., & Suzuki, H. (2012). Japan integrated velocity structure model version 1. *Paper presented at Proceedings of the 15th World Conference on Earthquake Engineering, Lisbon, Portual*. Sociedade Portuguesa de Engenharia Sismica. https://www.iitk.ac.in/nicee/wcee/article/WCEE2012_1773.pdf

Koper, K. D., Hutko, A. R., Lay, T., Ammon, C. J., & Kanamori, H. (2011). Frequency-dependent rupture process of the 2011 *Mw* 9.0 Tohoku Earthquake: Comparison of short-period P wave backprojection images and broadband seismic rupture models. *Earth Planets and Space*, *63*, 16. https://doi.org/10.5047/eps.2011.05.026

Larson, K. M., & Miyazaki, S. (2008). Resolving static offsets from high-rate GPS data: The 2003 Tokachi-oki earthquake. *Earth Planets and Space*, *60*, 801–808. https://doi.org/10.1186/BF03352831

Lay, T., & Kanamori, H. (1980). Earthquake doublets in the Solomon Islands. *Physics of the Earth and Planetary Interiors*, *21*, 283–304. https://doi.org/10.1016/0031-9201(80)90134-X

Lay, T., Liu, C., & Knamori, H. (2019). Enhancing tsunami warning using *P* wave coda. *Journal of Geophysical Research: Solid Earth*, *124*, 10583–10609. https://doi.org/10.1029/2019JB018221

Lay, T., & Rhode, A. (2019). Evaluating the updip extent of large megathrust ruptures using P_{coda} levels. *Geophysical Research Letters*, *46*, 5198–5206. https://doi.org/10.1029/2019GL082774

Lindquist, K. G., Engle, K., Stahlke, D., & Price, E. (2004). Global topography and bathymetry grid improves research efforts. *Eos, Transactions, American Geophysical Union*, *85*, 186. https://doi.org/10.1029/2004EO190003

Loveless, J. P., & Meade, B. J. (2016). Two decades of spatiotemporal variations in subduction zone coupling offshore Japan. *Earth and Planetary Science Letters*, *436*, 19–30. http://doi.org/10.1016/j.epsl.2015.12.033

Mavrommatis, A. P., Segall, P., & Johnson, K. J. (2014). A decadal-scale deformation transient prior to the 2011 *Mw* 9.0 Tohoku-oki earthquake. *Geophysical Research Letters*, *41*, 4486–4494. http://doi.org/10.1002/2014GL060139

Miura, S., Suwa, Y., Hasegawa, A., & Nishimura, T. (2004). The 2003 M8.0 Tokachi-Oki earthquake – How much has the great event paid back slip debts? *Geophysical Research Letters*, *31*, L05613. https://doi.org/10.1029/2003GL019021

Miyazaki, S., Larson, K. M., Choi, K., Hikima, K., Koketsu, K., Bodin, P., et al. (2004). Modeling the rupture process of the 2003 September 25 Tokachi-Oki (Hokkaido) earthquake using 1-Hz GPS data. *Geophysical Research Letters*, *31*, L21603. https://doi.org/10.1029/2004GL021457

Miyazaki, S., Segall, P., Fukuda, J., & Kato, T. (2004). Space time distribution of afterslip following the 2003 Tokachi-oki earthquake: Implications for variations in fault zone frictional properties. *Geophysical Research Letters*, *31*, L06623. https://doi.org/10.1029/2003GL019410

Murotani, S., Miyake, H., & Koketsu, K. (2008). Scaling of characterized slip models for plate-boundary earthquakes. *Earth Planets and Space*, *60*, 987–991. https://doi.org/10.1186/BF03352855

Murotani, S., Satake, K., & Fujii, Y. (2013). Scaling relations of seismic moment, rupture area, average slip, and asperity size for M~9 subduction-zone earthquakes. *Geophysical Research Letters*, *40*, 5070–5074. https://doi.org/10.1002/grl.50976

Nagai, R., Kikuchi, M., & Yamanaka, Y. (2001). Comparative study on the source processes of recurrent large earthquakes in Sanriku-oki region: the 1968 Tokachi-oki earthquake and the 1994 Sanriku-oki earthquake. *Zisin*, *54*, 267–280. https://doi.org/10.4294/zisin1948.54.2_267

Nanayama, F., Satake, K., Furukawa, R., Shimokawa, K., Atwater, B. F., Shigeno, K., & Yamaki, S. (2003). Unusually large earthquakes inferred from tsunami deposits along the Kuril trench. *Nature*, *424*, 660–663. https://doi.org/10.1038/nature01864

National Research Institute for Earth Science and Disaster Resilience. (2019a). *NIED K-NET, KiK-net*. National Research Institute for Earth Science and Disaster Resilience. https://doi.org/10.17598/NIED.0004

National Research Institute for Earth Science and Disaster Resilience. (2019b). *NIED F-net*. National Research Institute for Earth Science and Disaster Resilience. https://doi.org/10.17598/NIED.0005

Nishimura, T. (2006). Fault model of the 1952 Tokachi-oki earthquake induced from geodetic data. *Chikyu Monthly*, *28*, 441–447 (in Japanese).

Noda, H., Nakatani, M., & Hori, T. (2013). Large nucleation before large earthquakes is sometimes skipped due to cascade-up—Implications from a rate and state simulation of faults with hierarchical asperities. *Journal of Geophysical Research: Solid Earth*, *118*, 2924–2952. https://doi.org/10.1002/jgrb.50211

Park, S.-C., & Mori, J. (2007). Are asperity patterns persistent? Implication from large earthquakes in Papua New Guinea. *Journal of Geophysical Research*, *112*, B03303. https://doi.org/10.1029/2006JB004481

Romano, F., Piatanesi, A., Lorito, S., & Hirata, K. (2010). Slip distribution of the 2003 Tokachi-oki M_w 8.1 earthquake from joint inversion of tsunami waveforms and geodetic data. *Journal of Geophysical Research*, *115*, B11313. https://doi.org/10.1029/2009JB006665

Satake, K. (2017). Great earthquakes in the 17th century along the Kuril and Japan trenches. *Bulletin of the Earthquake Research Institute*, *92*, 31–47 (in Japanese with English abstract)

Satake, K., Hirata, K., Yamaki, S., & Tanioka, Y. (2006). Re-estimation of tsunami source of the 1952 Tokachi-oki earthquake. *Earth Planets and Space*, *58*, 535–542. http://doi.org/10.1186/BF03351951

Satake, K., Nanayama, F., Yamaki, S., Tanioka, Y., & Hirata, K. (2005). Variability among tsunami sources in the 17th-21st centuries along the southern Kuril Trench. In K. Satake (Ed.), Tsunamis. Advances in natural and technological hazards research (23). Dordrecht: Springer. https://doi.org/10.1007/1-4020-3331-1_9

Sawai, Y., Kamataki, T., Shishikura, M., Nasu, H., Okamura, Y., Satake, K., et al. (2009). Aperiodic recurrence of geologically recorded tsunamis during the past 5500 years in eastern Hokkaido, Japan. *Journal of Geophysical Research*, *114*, B01319. https://doi.org/10.1029/2007JB005503

Schurr, B., Asch, G., Hainzl, S., Bedford, J., Hoechner, A., Palo, M., et al. (2014). Gradual unlocking of plate boundary controlled initiation of the 2014 Iquique earthquake. *Nature*, *512*, 299–302. https://doi.org/10.1038/nature13681

Schwartz, S. Y. (1999). Noncharacteristic behavior and complex recurrence of large subduction zone earthquakes. *Journal of Geophysical Research*, *104*, 23111–23125. https://doi.org/10.1029/1999JB900226

Shinohara, M., Yamada, T., Kanazawa, T., Hirata, N., Kaneda, Y., Takanami, T., et al. (2004). Aftershock observation of the 2003 Tokachi-oki earthquake by using dense ocean bottom seismometer network. *Earth Planets and Space*, *56*, 295–300. https://doi.org/10.1186/BF03353054

Tanioka, Y., Hirata, K., Hino, R., & Kanazawa, T. (2004). Slip distribution of the 2003 Tokachi-oki earthquake estimated from tsunami waveform inversion. *Earth Planets and Space*, *56*, 373–376. https://doi.org/10.1186/BF03353067

Tanioka, Y., Nishimura, Y., Hirakawa, K., Imamura, F., Abe, I., Abe, Y., et al. (2004). Tsunami run-up heights of the 2003 Tokachi-oki earthquake. *Earth Planets and Space*, *56*, 359–365. https://doi.org/10.1186/BF03353065

Tanioka, Y., Satake, K., & Hirata, K. (2007). Recurrence of recent large earthquakes along the southernmost Kurile-Kamchatka subduction zone. In J. Eichelberger, E. Gordeev, P. Izbekov, M. Kasahara, & J. Lees (Eds.), Volcanism and subduction: The Kamchatka region (Vol. 172, pp. 145–152). Washington, DC: American Geophysical Union. https://doi.org/10.1029/172GM13

Tilmann, F., Zhang, Y., Moreno, M., Saul, J., Eckelmann, F., Palo, M., et al. (2016). The 2015 Illapel earthquake, central Chile: A type case for a characteristic earthquake? *Geophysical Research Letters*, *43*, 574–583. https://doi.org/10.1002/2015GL066963

Ueno, H., Hatakeyama, S., Aketagawa, T., Funasaki, J., & Hamada, N. (2002). Improvement of hypocenter determination procedures in the Japan Meteorological Agency. *Quarterly Journal of Seismology*, *65*, 123–134.

Utsu, T. (1999). *Seismicity studies: A comprehensive review*. Tokyo: Univ Tokyo Press (in Japanese).

Weatherall, P., Marks, K. M., Jakobsson, M., Schmitt, T., Tani, S., Arndt, J. E., et al (2015). A new digital bathymetric model of the world's oceans. *Earth and Space Science*, *2*, 331–345. https://doi.org/10.1002/2015EA000107

Wessel, P., & Smith, W. H. F. (1998). New, improved version of the Generic Mapping Tools released. *Eos Transactions, American Geophysical Union*, *79*, 579. https://doi.org/10.1029/98EO00426

Yagi, Y. (2004). Source rupture process of the 2003 Tokachi-oki earthquake determined by joint inversion of teleseismic body wave and strong ground motion data. *Earth Planets and Space*, *56*, 311–316. https://doi.org/10.1186/BF03353057

Yamada, T., Shinohara, M., Kanazawa, T., Hirata, N., Kaneda, Y., Takanami, T., et al. (2005). Aftershock distribution of the 2003 Tokachi-oki earthquake derived from high-dense network of ocean bottom seismographs. *Zisin*, *57*, 281–290 (in Japanese with English abstract). https://doi.org/10.4294/zisin1948.57.3_281

Yamanaka, Y., & Kukuchi, M. (2003). Source process of the recurrent Tokachi-oki earthquake on September 26, 2003, inferred from teleseismic body waves. *Earth Planets and Space*, *55*, e21–e24. https://doi.org/10.1186/BF03352479

Ye, L., Kanamori, H., Avouac, J.-P., Li, L., Cheung, K. F., & Lay, T. (2016). The 16 April 2016, MW 7.8 (MS 7.5) Ecuador earthquake: A quasi-repeat of the 1942 MS 7.5 earthquake and partial re-rupture of the 1906 MS 8.6 Colombia–Ecuador earthquake. *Earth and Planetary Science Letters*, *454*, 248–258. https://doi.org/10.1016/j.epsl.2016.09.006

Yokota, Y., & Koketsu, K. (2015). A very long-term transient event preceding the 2011 Tohoku earthquake. *Nature Communications*, *6*, 5934. https://doi.org/10.1038/ncomms6934

Yokota, Y., Koketsu, K., Fujii, Y., Satake, K., Sakai, S., Shinohara, M., & Kanazawa, T. (2011). Joint inversion of strong motion, teleseismic, geodetic, and tsunami datasets for the rupture process of the 2011 Tohoku earthquake. *Geophysical Research Letters*, *38*, L00G21. https://doi.org/10.1029/2011GL050098

Yoshida, S., Koketsu, K., Shibazaki, B., Sagiya, T., Kato, T., & Yoshida, Y. (1996). Joint inversion of near-and far-field waveforms and geodetic data for the rupture process of the 1995 Kobe earthquake. *Journal of Physics of the Earth*, *44*, 437–454. https://doi.org/10.4294/jpe1952.44.437

Zhu, L., & Rivera, L. A. (2002). A note on the dynamic and static displacements from a point source in multilayered media. *Geophysical Journal International*, *148*, 619–627. https://doi.org/10.1046/j.1365-246X.2002.01610.x

References From the Supporting Information

Abe, K. (1981). Magnitudes of large shallow earthquakes from 1904 to 1980. *Physics of the Earth and Planetary Interiors*, *27*, 72–92. https://doi.org/10.1016/0031-9201(81)90088-1

Akaike, H. (1980). Likelihood and the Bayes procedure. *Trabajos de Estadistica y de Investigacion Operativa*, *31*, 143–166. https://doi.org/10.1007/BF02888350

Alvarado, P., & Beck, S. (2006). Source characterization of the San Juan (Argentina) crustal earthquakes of 15 January 1944 (M_w 7.0) and 11 June 1952 (M_w 6.8). *Earth and Planetary Science Letters*, *243*, 615–631. https://doi.org/10.1016/j.epsl.2006.01.015

Charlier, C., & Van Gils, J. M. (1953). *Liste des stations seismologiques mondiales*. Uccle: Observatoire Royal de Belgique

Estabrook, C. H., Jacob, K. H., & Sykes, L. R. (1994). Body wave and surface wave analysis of large and great earthquakes along the Eastern Aleutian Arc, 1923–1993: Implications for future events. *Journal of Geophysical Research*, *99*, 11643–11662. https://doi.org/10.1029/93JB03124

Geller, R. J., & Kanamori, H. (1977). Magnitudes of great shallow earthquakes from 1904 to 1952. *Bulletin of the Seismological Society of America*, *67*, 587–598.

Goodstein, J. R., Kanamori, H., & Lee, W. (1980). Seismology microfiche publications from the Caltech Archive. *Bulletin of the Seismological Society of America*, *70*, 657–658.

Gutenberg, B. (1945). Amplitudes of surface waves and magnitudes of shallow earthquakes. *Bulletin of the Seismological Society of America*, *35*, 3–12.

Gutenberg, B., & Richter, C. F. (1942). Earthquake magnitude, intensity, energy, and acceleration. *Bulletin of the Seismological Society of America*, *32*, 163–191.

Gutenberg, B., & Richter, C. F. (1954). *Seismicity of the Earth and related phenomena*. Princeton, NJ: Princeton University Press

Gutenberg, B., & Richter, C. (1955). Magnitude and energy of earthquakes. *Nature*, *176*, 795. https://doi.org/10.1038/176795a0

Hamamatsu, O. (1966). Historical table of seismographs for routine observations JMA network. *Zisin*, *19*, 286–305 (in Japanese with English abstract). https://doi.org/10.4294/zisin1948.19.4_286

Kanamori, H., & Ross, Z. E. (2019). Reviving m_B. *Geophysical Journal International*, *216*, 1798–1816. https://doi.org/10.1093/gji/ggy510

Lienkaemper, J. (1984). Comparison of two surface-wave magnitude scales: M of Gutenberg and Richter (1954) and Ms of "Preliminary Determination of Epicenters". *Bulletin of the Seismological Society of America*, *74*, 2357–2378.

Sapporo Regional Headquarters, & Obihiro Meteorological Station. (1962). A report of the Hiroo-oki earthquake on April 23, 1962. *Quarterly Journal of Seismology*, *27*, 69–77.

Vanek, J., Zatopek, A., Karnik, V., Kondorskaya, N., Riznichenko, Y. V., Savarensky, E., et al. (1962). Standardization of magnitude scales. *Bulletin of the Academy of Sciences of the USSR Geophysics Series*, *2*, 108–111.